C H A P T E R - 6

Characterization of tungsten diselenide (n-WSe_2)/electrolyte interface.

SARDAR PATEL UNIVERSITY
BHAIKAKA
LIBRARY
Vallabh Vidyanagar

6.1. INTRODUCTION :

For binding a suitable photoactive,but stable semi-conducting material, a systematic search for appropriate new type of electrodes for electrochemical solar cells had been initiated. The basic idea was that the visible light phototransition should not be an electron transition from an valence band to the cation conduction band which is a characteristic of polar semiconductors such as CdS, GaAs or GaP and breaks a polar bond but that it should occur between energy bands resulting from d-orbitals of the metal component of the semi-conductor. The investigation consequently centered on transition metal dichalcogenides (TMDC's) with the problem of finding those compounds with a maximum of d-d splitting which could be necessary for the absorption of photons of energy about 2 ev (1-15). Such materialswere found to be tungstendisulphide and molybdenum disulphide. The photoelectrodes constructed from these compounds are found to be stable to photocorrosion reaction over extended periods.

In general, the properties like band gap energy, band positions and stability to corrosion are the parameters of interest, which effect the conversion efficiency (16,17).

Keeping this in view author has made attempts to fabricate the photoelectrochemical solar cells using the grown crystals of WSe_2 and characterize them optically and electrochemically. Determination of optical band gap from spectral response and flat band potentials in the present work on n-WSe_2 have been made by capacitance measurement from Mott-Schottky plots. This chapter describes the observations thus made.

6.2. EXPERIMENTAL :

Single crystals of tungsten diselenide grown by chemical vapour transport (CVT) technique, using bromine, tellurium tetrachloride and selenium tetrachloride with an excess amount of selenium transporting agents have been used in the present work. From Hall effect measurements it was ascertained that all these crystals were n-type semi-conductors.

6.2.1. SOLAR CELL FABRICATION :

A glass tube with a fine bore and flattend end was used for mounting the single crystals. A copper wire was introduced thrugh the bore and connected to the crystals using a highly conducting silver paste. The electrode surface was insulated at the edges using a good epoxy. The semiconductor electrode was then immersed in an aqueous iodine/iodide electrolyte

by mixing 1M NaI and 0.05 M I_2 in doubly distilled water and platinum grid was used as a counter electrode.

6.2.2. SPECTRAL RESPONSE MEASUREMENTS :

The experimental set up for the spectral response measurement of PEC cell configuration is as shown in Fig. 6.1. It consists of a grating monochromator (Central Electronic Ltd., India), a PEC cell using n-WSe_2 electrode and a digital multimeter (Agronic 67, India). PEC cell has been illuminated by monochromatic light from a monochromator and spectral response has been observed for wave lengths 910nm to 500 nm at an interval of 10 nm.

6.2.3. CAPACITANCE MEASUREMENTS :

Capacitance measurements were made by using the LCR meter (VLCR-27, Vasavi Electronics, India). A saturated colomel electrode (SCE) was employed as a reference electrode to measure the potential applied to the semiconductor electrode. A schematic diagram representing the experimental set up of PEC cell for capacitance measurements is shown in Fig. 6.2.

6.3. RESULTS AND DISCUSSION :

The spectral dependence of the photocurrent of n-WSe_2 on the wavelength of incident light is shown in Fig. 6.3. In all cases the output photocurrent gradually drops absorption in the semiconductor continues to increase. The decrease in spectral response towards the long-wavelength region may be attributed to the fact that an increasing fraction of photons was absorbed beyond the region determined by space charge layer plus the diffusion length of holes so that corresponding electron-hole pairs get lost by recombination (18). The decrease in the spectral response at short wavelengths is due to the recombination in the surface region where recombination in the surface region where recombination is highest. According to De Angelis etal (19) the wave length dependence of photocurrent was explained by taking into account the depletion layer width, light penetration depth, and thickness of sample. It was suggested by Tributsch (12) that the photocurrent of TMDC's essentially arises from direct d-d transitions.

The semiconductor-electrolyte interface can be treated as a Schottky barrier (14) and the photocurrent has the following behaviour.

$$J = e\phi_o \left[1 - \frac{\exp\left\{-\alpha W_o (V-V_{fb})^{1/2}\right\}}{1 - \alpha L_p}\right] \qquad \ldots.(6.1)$$

where, ϕ_o is the photon flux, L_p is the hole diffusion length, V_{fb} is the flat band potential, α is the optical absorption coefficient and W_o is the characterstic depletion layer width. W_o is given by $(2\epsilon / e N_D)^{1/2}$ where, ϵ is the dielectric constant, e is the electronic charge and N_D the donar density.

It has been shown that the optical absorption for inter band transitions in a semiconductor close to the gap behaves as

$$\alpha = \frac{A (h\nu - E_g)^{n/2}}{h\nu} \quad .....(6.2)$$

where, n = 1 for direct and n=4 for indirect transitions. These two equations completely describe the photoresponse of the semiconductor-electrolyte junction.

It has been suggested by Lemasson etal (20) that the photo-response is directly proportional to the photon flux and Radon and Vigneron (21) that the photocurrent is proportional to absorption spectrum. The plots of $(Jh\nu)^{1/2}$ versus $h\nu$ (Fig.6.4(a,b,c). for the tunsten diselenide are straight lines (n=1) indicating that these materials are direct band gap semicnductors. The values of optical band gaps obtained from $(Jh\nu)^{1/2}$ versus $h\nu$ plots have been given in Table 6.1 which shows good agreement with the

with the reported values (28,29).

From the semi-conductor-electrolyte interface shown in Fig. 6.5, it can be noted that there are two capacitors in series across the interface (14). One is the Helmholtz layer capacitor in the electrolyte near the interface, C_H and the other is the depletion layer capacitor formed in the semiconductor near the interface, C_{sc}. Since $C_H >> C_{sc}$, the net effective capacitance across the interface is C_{sc}. The depletion layer capacitance, C_{sc}, is known to vary with bias applied to the semiconductor. This variation is given by the Mott-schottky relation, (22,23).

$$\frac{1}{C_{sc}^2} = \frac{2}{\epsilon \epsilon_o e N_D} \left[| V_{SCE} | - \frac{KT}{e} \right] \quad \ldots(6.3)$$

where, ϵ is the dielectric constant, ϵ_o the permitivity of free space, e the charge of electron, N_D, donar concentration, V_{SCE} applied potential across the space charge layer which can be expressed as, $V_{SCE} = V - V_{fb}$, V_{fb} is the flat band potential. From equation (6.3) it is seen that a straight line would be obtained if $1/C_{sc}^2$ versus V is plotted. This intercept on the V axis gives the flat bandpotential V_{fb} and from the slope of the curve the value of donar concentration N_D can be calculated.

Mott-schottky plot of n-WSe_2 single crystal at 1 KHZ frequency in 1M NaI and 0.05M I_2 is shown in Fig.6.6 (a,b,c). The flat band potential V_{fb} evaluated from the plots are 0.37V, 0.36V and 0.33 V versus V_{SCE}, for the crystal grown by Br_2, $TeCl_4$ and $SeCl_4$ + Se respectively. These are all in good agreement with the values reported earlier (24). The donar concentration N_D, was determined from the slope of Mott-Schottky relation.

$$N_D = [2e\epsilon\epsilon_o (\text{Slope})]^{-1} \quad \ldots\ldots\ldots(6.4)$$

Where, ϵ is the dielectric constant of the crystal. The dielectric constants of WSe_2 crystals have been evaluated using the relation $\epsilon = cd/A\epsilon_o$, where, C is the capacitance, d is the thickness of the crystal and A is the area of contact. The donar concentration N_D, calculated using above relations are shown in Table 6.1.

The distance between conduction band minimum, E_c, and flat band potential, V_{fb} is important to localize the valence band maximum.

According to kautek and Gerischer (25) in classical approximation where $(E_c - E_{fb})/ KT > 1$, the effective density of conduction states is given by (26)

$$N_c = \frac{2}{h^3} (2\pi m_e^* KT)^{3/2} \quad \ldots\ldots\ldots\ldots(6.5)$$

where, m_e^* is the effective mass of electron and is taken to be 0.5 m_e (27), m_e being the electron mass. For TMDC's N_c comes out to be 8.8 x $10^{18} cm^{-3}$. Assuming that all donars are ionised and have given their electrons into the conduction band, we get the classical Maxwell Boltzmann distribution.

$$E_c - E_{fb} = KT \ln (N_C/N_D)) \quad \text{.....(6.6)}$$

$$E_c - E_{fb} = -e (V - V_{fb}) \quad \text{.....(6.7)}$$

Using these equations author has obtained the difference between the fermi level and the edge of conduction band $(E_c - E_{fb})$ for WSe_2 as shown in Table 6.1. By substracting the band gap energy for WSe_2 given in Table.6.1. from the value of E_c, the conduction band, the valence band and positions, E_v, have been located as depicted in Fig. 6.7. This figure suggests that the redox potential V_{redox} within the gap i.e. + Ve of - 0.55 V and - Ve of + 1.2 V versus V_{SCE} should be appropriate for PEC cells with tungsten diselenide electrodes.

6.4. CONCLUSION :

The n-type semiconducting nature of WSe_2 crystals has been confirmed from Hall coefficient and Mottschottky plots. n-WSe_2 electrodes have been characterized in terms of the energetic location of the valence and conduction band positions, which suggests that the redox potentials with the gap,

positive of-0.55V and negative of + 1.2 versus V_{SCE} should be appropriate for PEC solar cells of n-type tungsten diselenide single crystal electrodes, in iodine/iodide electrolyte. The direct band gap of the grown crystals are lying between 1.56 ev and 1.65 ev.

TABLE 6.1.

OBTAINED DATA FROM MOTT-SCHOTTKY AND SPECTRAL RESPONSE

EVALUATIONS FOR n-WSe_2 ELECTRODES

Crystals grown by the transporter	Donar Concentration N_D Cm^{-3}	$E_c - E_f$ V. V_S. V_{SCE}	V_{fb} V. V_S. V_{SCE}	E_V V. V_S. V_{SCE}	Band gap eV
Br_2	2.5668×10^{16}	0.1512	-0.370	1.0388	1.56
$TeCl_4$	2.4493×10^{16}	0.1524	-0.360	1.0676	1.58
$SeCl_4$ + Se	1.9654×10^{16}	0.1581	-0.330	1.1619	1.65

R E F E R E N C E S

1. Tributsch. H., 1977,
Z. Naturforsch Teil., A32, 972.

2. Tributsch. H, 1981,
J.Electrochem. Soc., 128, 1261.

3. Tributsch H. and Bennet J.C., 1977,
J.Electroanal chem. Interfacial Electrochem.,
81, 97.

4. Lewernz H.J., Heller A and Disalve F.J., 1980,
J. Am. Chem. Soc., 102, 1887.

5. Menezes. S., Disalve F.J., and Miller B, 1980,
J. Electrochem Soc., 127, 1751.

6. White H.S., Fan F.R.F., and Bard A.J., 1981,
J.Electrochem. Soc., 128, 1045.

7. Nagasubramanian G. and Bard A.J., 1981,
J.Electrochem Soc., 128, 1055.

8. Canfield D. and Parkinson B.A., 1981,
J. Am. Chem. Soc., 103, 1279.

9. Schneemeyer L.F., Wrighton M.S., Stacy A and
Sienko. M.J., 1980,
Appl. Phys., Lett., 36, 701.

10. Fan F.R.F., white H.S. Wheeler B and Bard A.J.,
1980,
J.Electrochem Soc., 127, 518.

11. Kline G., Kam. K, Canfield D and Parkinson
B.A., 1981.
Solar Energy Mater., 4, 301.

12. Tributsch H, 1977,
Ber. Bunsenges Phys., Chem., 81, 361.

13. Loferski J.J., 1950,
J.Appl. Phys., 27, 777.

14. Butler M.A. and Ginley D.S., 1980,
J. Mater Sci., 15, 1.

15. Sinha. A.P.B., 1983,
Energy Digest (India)., 2,1.

16. Gerischer H., 1977,
J.Electroanal Chem., 82, 133.

17. Bard. A.J., and Wrighton M.S., 1977,
J.Electrochem. Soc., 124, 1706.

18. Van Merhaeghe R.L. and Cardon F., 1979,
Ber. Bunsenges phys. chem., 83,236.

19. De Angelis. L., Scafe E., Gulluzi. F.,
Fornarinin L and Scrosati. B, 1982,
J.Electrochem Soc., 129, 237.

20. Lemasson P., Etcheberry A and Goutron J, 1983,
Electrochimica Acta., 27, 607.

21. Redon A.M, and Vigneron. J, 1981,
Solar Cells., 3, 179.

22. Schottky. W., 1939,
Z Phys., 113, 367.

23. Mott. N.F., 1939
Proc. Roy. Soc., A 171, 27.

24. Kautek W. and Gerischer. H, 1982,
Electrochimica Acta., 27, 355.

25. Kautek W. and Gerischer H., 1980,
Ber Bunsenges. phys. chem., 84, 645.

26. Gerischer H, 1961,
Adv., Electrochem. Engang., 1, 139.

27. Wilson J.A. and Yoffe A.D., 1969,
Adv. Phys., 18, 193.

28. Gobrecht. J. Gerischer H and Tributsch. H,
1978,
Ber Bunsenges Phys. Chem., 82, 1331.

29. Baglio. J.A., Calabrese G.S.Kamieniecki. K,
Kershaw R, Kubiak C.P., Ricco A.J. wood. A.,
Wrighton M.S. and Zoski G.D. 1982,
J.Electrochem. Soc., 129, 1461.

CAPTIONS OF THE FIGURES :

Fig.6.1. Photograph of the experimental set up for spectral response measurements.

Fig.6.2. Schematic diagram of experimental set up of PEC cell for capacitance measurement.

Fig.6.3. Plots of photocurrent versus wavelength for tungsten diselenide electrodes.

Fig.6.4. (a,b andc) $(Jh\nu)^2$ versus $h\nu$ plots of n-WSe_2 grown by Br_2, $TeCl_4$ and $SeCl_4$ + Se transporters respectively.

Fig.6.5 The potential and charge distribution at the semiconductor-electrode interface (ϕ is the potential), Q the charge)

Fig.6.6. (a,b and c) Mott-Schottky plots of n-WSe_2 grown by Br_2, $TeCl_4$ and $SeCl_4$ +Se transporters in aqueous iodine/iodide electrolyte respectively.

Fig.6.7 Positions of band edges of n-WSe_2 in aqueous iodine/iodide electrolyte, E_c, conduction band E_v, Valence band, E_f, fermi level.

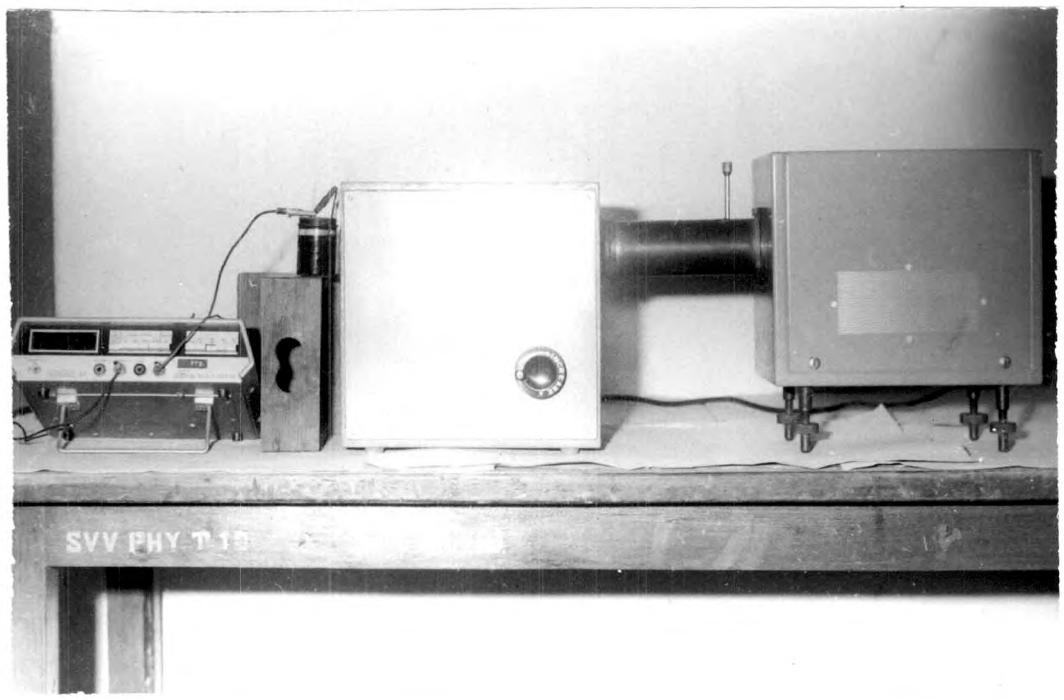

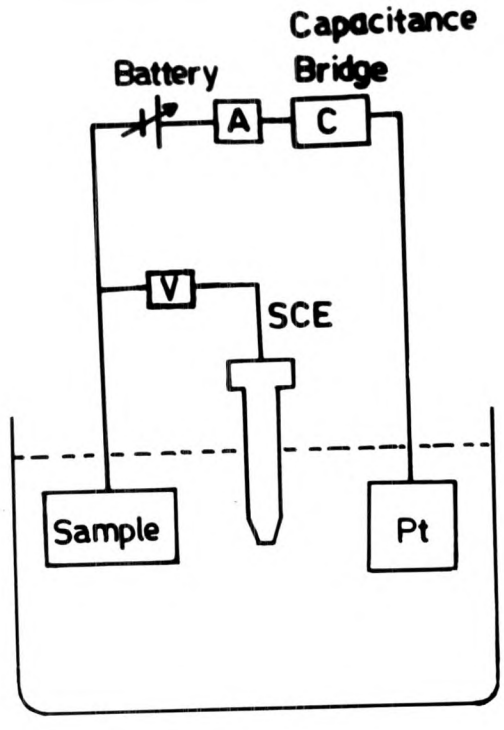

FIG·6·1

FIG·6·2

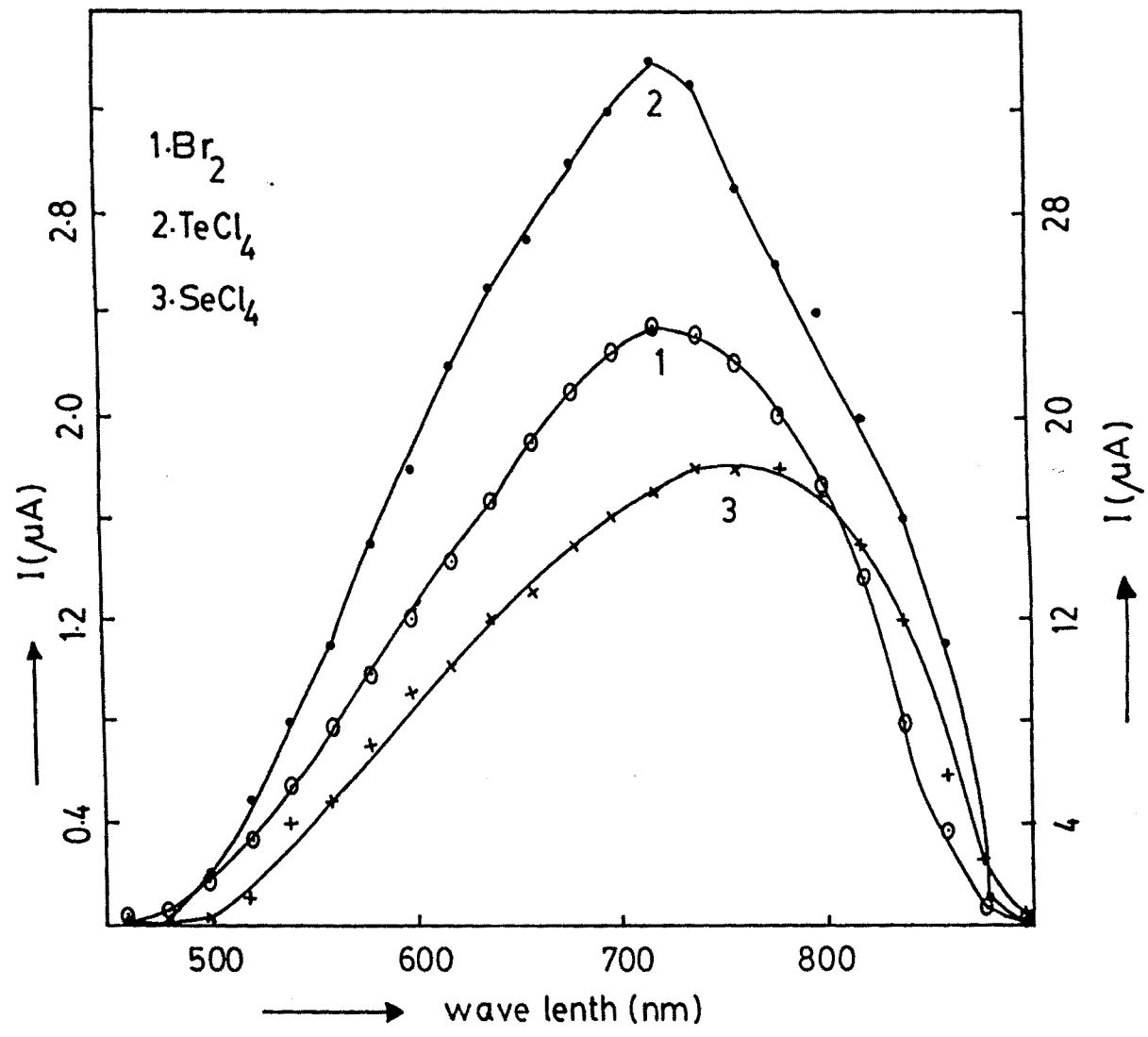
1·Br2
2·TeCl4
3·SeCl4
I(μA)
0·4
1·2
2·0
2·8
4
12
20
28
I(μA)
500
600
700
800
wave lenth (nm)

FIG·6.3

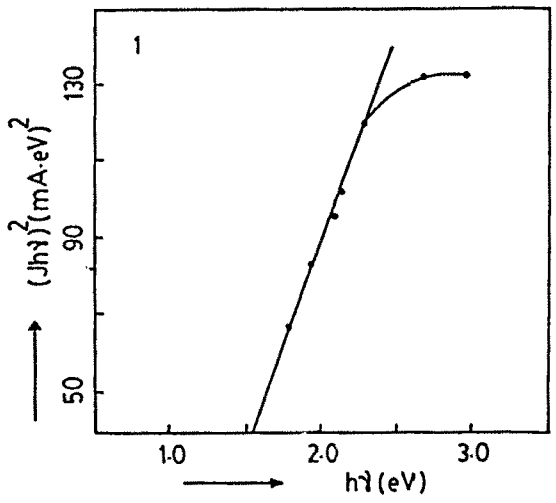

FIG.6.4(a)

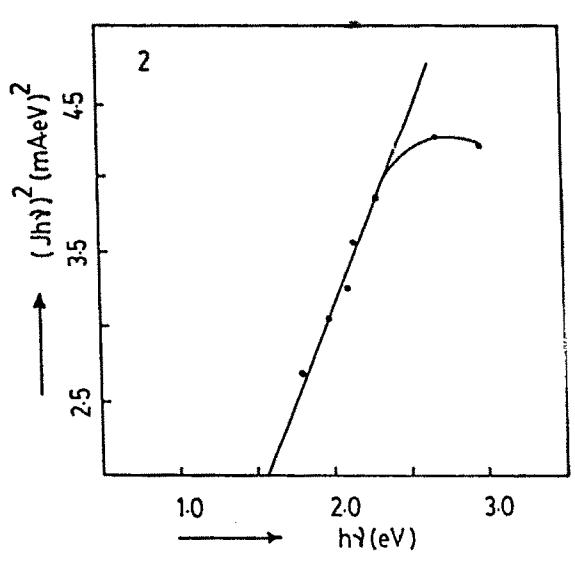

FIG.6.4(b)

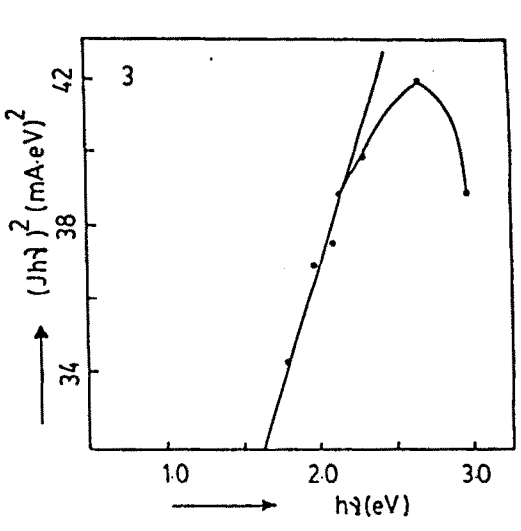

FIG.6.4(c)

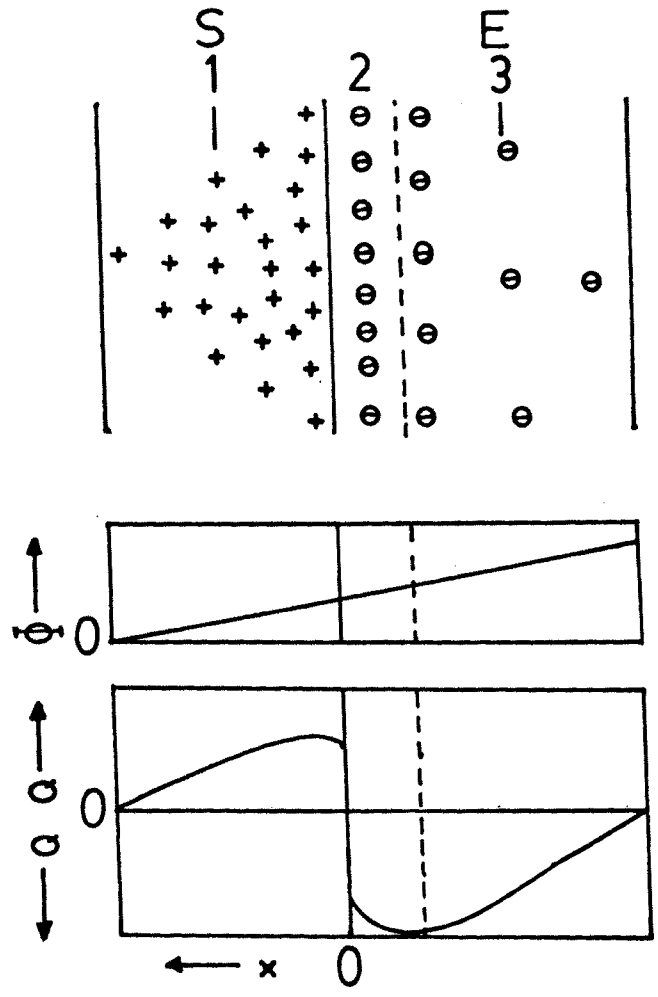

S·semiconductor
E·electrolyte
1·space charge region
2·1st Helmholtz layer
3·Gouy layer

FIG·6·5

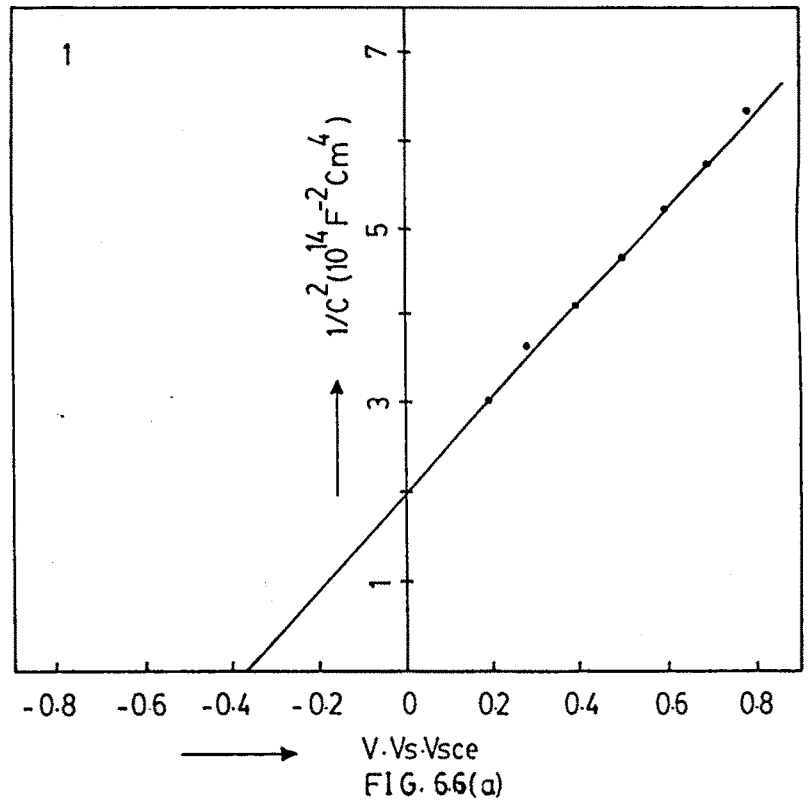

FIG. 6.6(a)

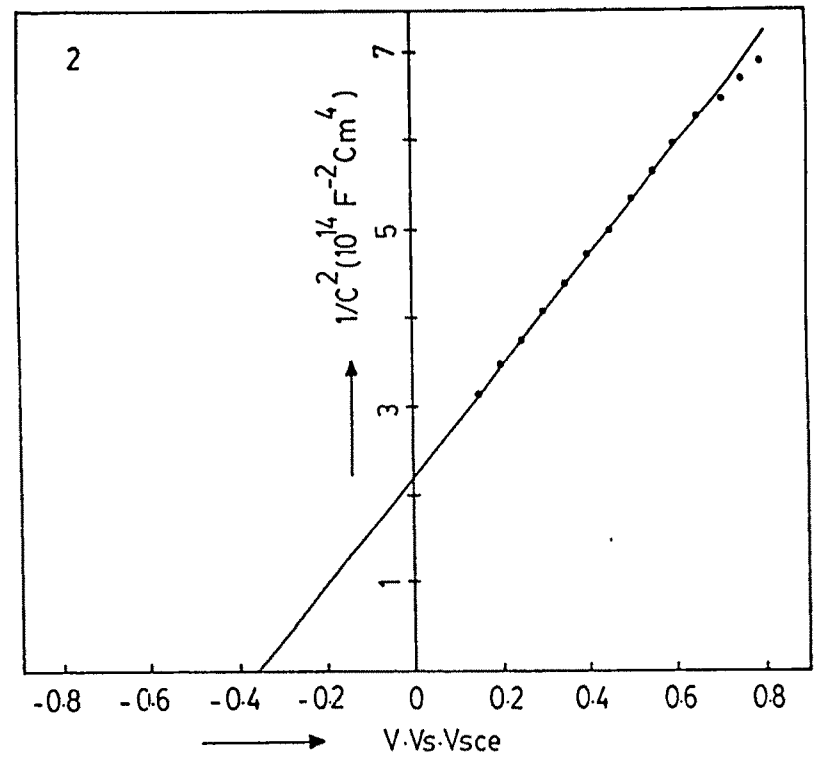

FIG. 6.6(b)

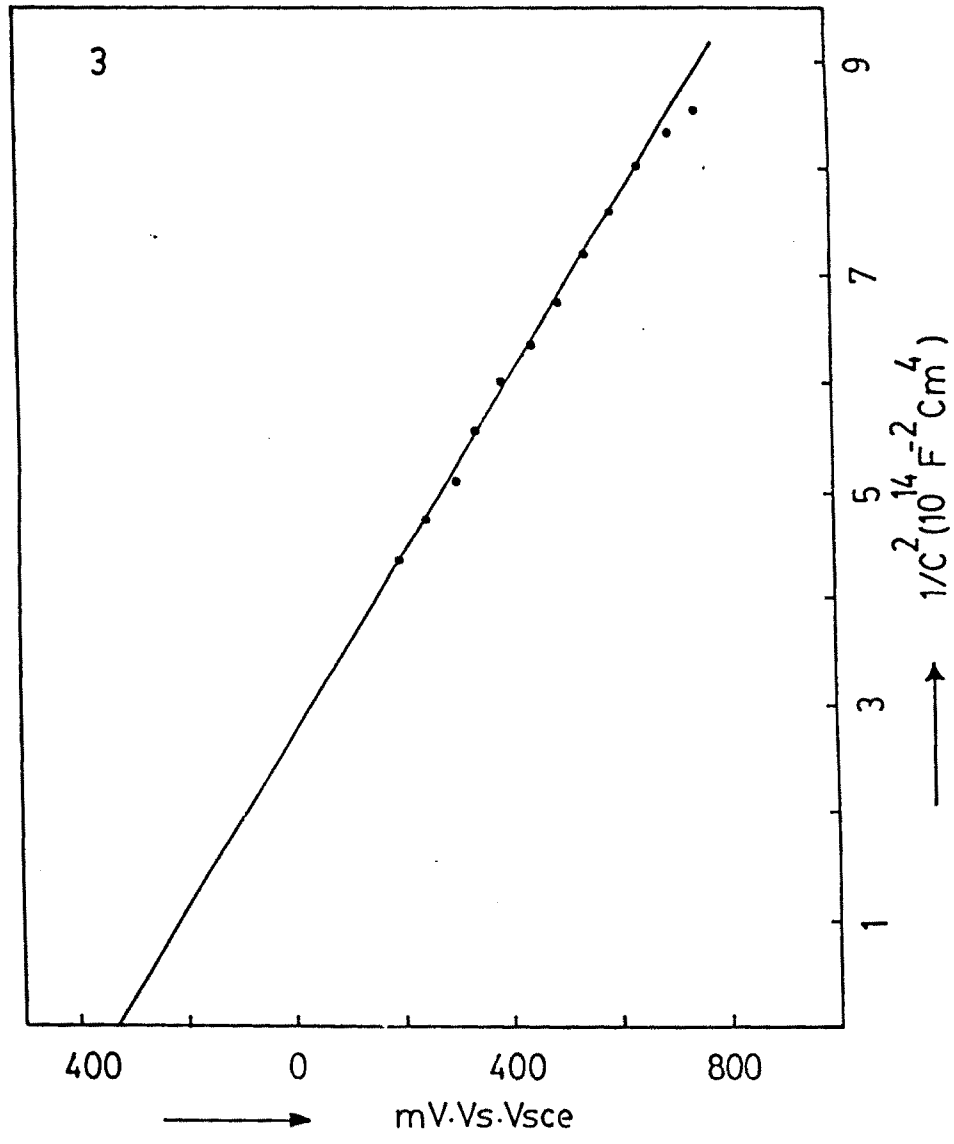

FIG·6·6(c)

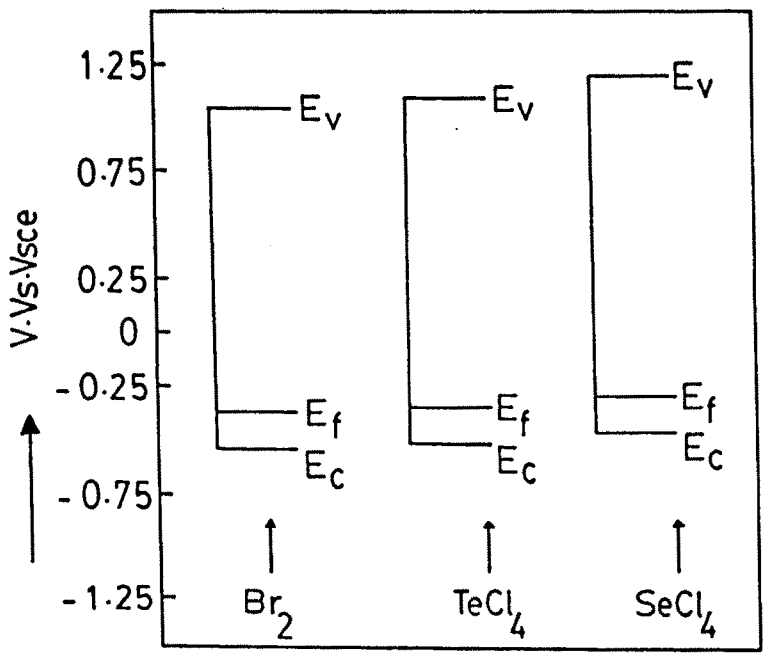

FIG·67